J4.9

A Generalized Inversion Scheme for GPS Occultation Data Taken by a Receiver Inside or Outside the Atmosphere

Cinzia Zuffada*, George Hajj and E. Robert Kursinski

Jet Propulsion Laboratory
California Institute of Technology
Pasadena, CA 91109

1. INTRODUCTION

Radio occultation measurements using the Global Positioning System (GPS) and a receiver in low-Earth orbit (LEO) have recently been shown to provide accurate profiles of atmospheric refractivity, pressure, water vapor and temperature with high vertical resolution [e.g. Kursinski et al., 1996]. When a GPS transmitter and receiver pair are on opposite sides of the atmosphere, the radio signal propagating in the intervening medium is bent due to the atmospheric refractivity gradient. The bending creates a Doppler frequency shift in the received signal and can therefore be obtained directly from the GPS observable. Assuming a spherically symmetric atmosphere, the bending can be expressed as a function of refractivity by an integral equation. When the receiver is located outside the atmosphere, this equation can be inverted via an Abelian integral transformation to generate vertical profiles of refractivity, from which temperature, pressure and water vapor can be derived.

A more general inversion scheme is desirable to account for the effects of nonspherical structure and thereby improve accuracy. Even for the spherically symmetric case, the Abelian transformation cannot be used when a receiver is located within the atmosphere. A more general inversion scheme could utilize GPS measurements from a mountain top or an airplane tracking the GPS signal down to the Earth's limb. Such "down-looking" receivers could routinely yield 10's of daily profiles in regions of interest, providing much needed vertical information on boundary layer structure. In particular, water vapor density below the receiver's height in the surrounding region could be obtained with a vertical resolution of a couple hundred meters.

We present a generalized raytracing inversion scheme which can be used when the occultation data is taken from within or outside the atmosphere. In this scheme, spherical symmetry is retained and the refractivity is modeled as piecewise exponential, with scale height changing from one atmospheric layer to the next. Continuity of refractive index is insured at the layer boundaries, while the derivatives are allowed to jump. The exponential scale heights and a normalizing value of refractivity are retrieved by minimizing, in a least square sense, the residuals between measured bending angles and those calculated based on the exponential model.

We also present results comparing refractivity and temperature profiles obtained by this generalized raytracing scheme against those derived via the Abel inversion for the GPS/MET experiment and for a hypothetical situation where the receiver is placed within the atmosphere. Our technique can be applied to assimilate GPS occultation data into numerical weather models.

2. INVERSION SCHEMES

Based on geometrical optics, a signal traveling in a spherically symmetric medium will bend by an amount

$$\alpha = a \int_{raypath} \frac{1}{n\sqrt{n^2 r^2 - a^2}} \frac{dn}{dr} \qquad (1)$$

*C. Zuffada - Jet Propulsion Laboratory, 4800 Oak Grove Dr., MS 238-600, Pasadena, CA 91109
e_mail: cinzia@yellowstone.jpl.nasa.gov

where *r* is a point along the raypath, n is the index of refraction at *r,* and *a* is the impact parameter. (We distinguish between *N* and *n, we* call the former refractivity and the latter index of refraction which are related by $N = (n-1) \times 10^6$).

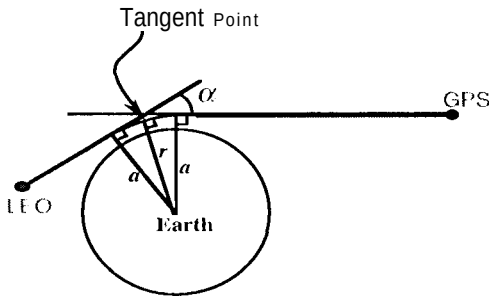

Fig. 1: The geometry of GPS occultation when the receiver is outside the atmosphere.

GPS satellites transmit L1 (19.0 cm) and L2 (24.4 cm) carrier signals modulated by a pseudo-random code. The observable acquired during an occultation are measurements of the L1 and L2 phase delays between the transmitter and the receiver. From knowledge of the positions of the transmitter and the receiver and their clocks, the delay due to the intervening media can be isolated. Both L1 and L2 signals are used to calibrate for the dispersive ionosphere, and the extra neutral atmospheric delay is isolated. (For a more detailed discussion of how atmospheric delay is detected see e.g. Hajj et al., (1 995).) From knowledge of the atmospheric extra delay as a function of time, we can derive the extra atmospheric Doppler which can be related to the bending of the signal via the equation

$$\Delta f = \frac{f}{c}\left(\vec{v}_t \cdot \vec{k}_t - \vec{v}_r \cdot \vec{k}_r - \{\vec{v}_t - \vec{v}_r\} \cdot \vec{k}\right) \qquad (2)$$

where *f* is the GPS transmitting frequency, c is the speed of light, $\vec{v}_t$ and $\vec{v}_r$ are the transmitter and receiver velocities, respectively, k, and $\vec{k}_r$ are the unit vectors in the direction of the transmitted and received signal, respectively, and $\vec{k}$ is the unit vector in the direction of the straight line passing through the transmitter and receiver positions. From Eq. (2) and the requirement that bending be equal on both sides of the tangent point (which is dictated by the spherical symmetry assumption), the bending, *a,* can be derived as a function of the impact parameter, *a.* One GPS occultation data point is normally collected every 0.02 second (such as in GPS/MET experiment) but they are smoothed to the time it takes the tangent point to move by a Fresnel zone, which varies between 200-1500m depending on the height of the tangent point. These smoothed α's serve as the basic measurements to be inverted to obtain refractivity as described below.

2.1 Abel Inversion Scheme

The Abel inversion has been used extensively in seismic inversions as well as in inverting planetary occultation data [see e.g. Fjeldbo et al., 1971]; therefore, we describe it here very briefly and point out its limitations. Once the bending is determined, then Eq. (1) can be inverted with an Abelian transformation [e.g. Tricomi, 1977] to solve for *n* as

$$\ln(n(a)) = \frac{1}{\pi}\int_a^\infty \frac{\alpha(a')}{\sqrt{a'^2 - a^2}}\, da' \qquad (3)$$

Note that the integration in Eq. (3) extends to infinity, which makes it necessary to have measurements starting from outside of the atmosphere for this inversion to be performed. When the receiver lies inside the atmosphere, for instance when it is located on top of a mountain, the Abel integral transform of Eq. (3) cannot be applied because the bending is known only at a number of heights limited by that of the receiver location, which is then insufficient to perform the integral.

2.2 Raytracing Inversion Technique

The technique we present here is a raytracing technique which can be used to invert Eq. (1) for situations when the receiver is inside or outside the atmosphere. The steps followed in this technique are summarized below:

(1) Starting with $\{a,(a), i = 1, m_\alpha\}$ measurements we divide the atmosphere into m_α layers such that a layer is centered at the tangent height of each *a,* measurement. (Even though α_i is

given as a function of *a,* , the radius of the tangent point corresponding to that measurement, and therefore its height, is estimated by solving the relation $a = r\, n(r)$ where $n(r)$, the index of refraction at *r , is* obtained from an *a priori* model as a first guess).

(2) When the receiver is inside the atmosphere, we complement the set of α measurements with a set of values for refractivity above the receiver {N, , i=l ,m_n). These values are obtained from an *a priori* model and are chosen at heights commensurate with the levels of the *a priori* model. We add m_n additional layers to those of step (1) centered at these heights.

(3) We assume refractivity to be changing exponentially with a constant scale height within each layer. In what follows we will refer to this layering of the atmosphere as the "exponential model" (to distinguish it from the *a priori* model). This exponential model, therefore, consists of $m_L = m_\alpha + m_n$ layers, with m_L scale heights. Given these scale heights, and constraining the refractivity (but not its derivative) to be continuous across the boundaries of different layers, we can write a functional form that describes refractivity everywhere in the atmosphere as a function of *r,* the radial distance from the earth's center to a point in layer *j* , where $R_{j+1} > r > R_j$, as

$$N(r) = N_{norm} \exp\left(-\frac{r - R_j}{H_j}\right) \prod_{i=j+1}^{m_L} \exp\left(-\frac{\Delta_i}{H_i}\right) \tag{4}$$

where R_j is the lower boundary of the j^{th} layer, *A,* and *H,* are the i^{th} layer thickness and scale height, respectively. In Eq. (4) we introduce one additional parameter, the normalization factor of refractivity, N_{norm}. Because of this additional parameter, one additional refractivity value is obtained the *a priori* model to make the problem determined. Initial values of N_{norm} and *H,'s* are obtained from the *a priori* model.

(4) Eq. (4) represents our model for atmospheric refractivity. Values of $\{H_i , N_{norm}\}$ are then solved for, in a least square sense, to fit the m_α measurements of bending and the complementary m_n value of N. Because the problem is non-linear, several iterations are required before a solution is reached. At each iteration, *k,* we use the set{ H_i^k, N_{norm}^k }, Eq. (4) and Eq. (1) to calculate the bending and refractivity. We use the subscript c to indicate these computed quantities in the following equations. The calculated *a* and N are then difference from the observed bending and refractivity. Moving from one iteration to the next is accomplished by Taylor expanding around { H_i^k, N_{norm}^k }, To first order, this can be expressed as

$$\alpha_m = \alpha_c(H_i, N_{norm}) + \sum \frac{\partial}{\partial p} \alpha_c(H_i, N_{norm}) \Delta p$$

$$N_m = N_c(H_i, N_{norm}) + \sum \frac{\partial}{\partial p} \mathrm{NC}(H_i, N_{norm}) \Delta p$$

$$where \quad p = \{H_i, N_{norm}\} \tag{5}$$

Because of the non-linearity of the problem, it is beneficial to place some constraints on the allowed range of variation of Δp, so that the solution does not deviate very drastically from the previous point. This is accomplished by first not allowing *p* to change by more than a certain amount at a given iteration (0.2 km for the scale height and 20% of the last value of N_{norm}) and, second, by introducing an *a priori* information matrix, taken to be diagonal and such that

$$\Lambda_i = \frac{1}{\mathrm{cov}(p)} \qquad p = \{H_i, N_{norm}\} \tag{6}$$

where cov( ) indicates the parameter covariance. It can be shown [Bierman, 1977] that the introduction of the information matrix can be interpreted as the addition of extra measurements, corresponding to the equation

$$\sqrt{\Lambda_i}\, \Delta p = \mathrm{O} \tag{7}$$

In our inversion, the covariance cov(*p*) *is* taken to be very large; therefore, the extra measurements of Eq. (7) have no effect o n the solution; nevertheless, introducing such measurements is crucial for the regularization of this highly non-linear and ill-conditioned problem.

The problem to be solved is cast into a matrix form which can be represented compactly as

$$\begin{pmatrix} \Lambda_i \\ partial(\alpha) \\ partial(N) \end{pmatrix} \{ \Delta p \} = \begin{pmatrix} 0 \\ (\alpha_m - \alpha_c) \\ (N_m - N_c) \end{pmatrix} \quad (8)$$

On the left-hand side of Eq. (8) the overall problem matrix is composed of a diagonal submatrix and two matrices, normally upper triangular except for a few rows, obtained by calculating the partial derivatives of bending and refractivity with respect to $\{H_i, N_{norm}\}$. On the right-hand side of Eq. (8) are the discrepancies between measured and calculated α and N. The square root information filter [Bierman, 1977] is used to solve Eq. (8).

The examples shown below the starting values of$\{ H_i^0, N_{norm}^0 \}$ are derived from an *a priori* model which is taken to be either the National Meteorological Center (NMC) stratospheric model or the European Center for Medium-range Weather Forecasts (ECMWF) numerical weather analysis available every six hours.

At each new iteration, the tangent point radius, r_{min}, associated with a given α is obtained by recursively solving $a(r_{min}) = n(r_{min}) x r_{min}$ using the latest solution. Knowledge of r_{min} is needed to recompute the bendings (Eq. 1) and the partials (Eq. 5). Even though, the r_{min}'s can be changing as we iterate, the boundaries of the layers are fixed, and they are based on the initial layering scheme explained in steps (1) and (2).

3. **PRELIMINARY RESULTS**

3.1 Receiver Inside The Atmosphere

The first step in the validation of our technique, here referred to as ALPHA inversion, consists of reproducing some refractivity profiles which have been derived before with the Abel approach. We use data obtained from GPS/MET, an experiment which started in April of 1995 and placed a GPS receiver in low-Earth orbit taking the first GPS occultation data [Ware et al., 1996]. We illustrate the comparisons in Figs. 2, 3 and 4, for one particular occultation.

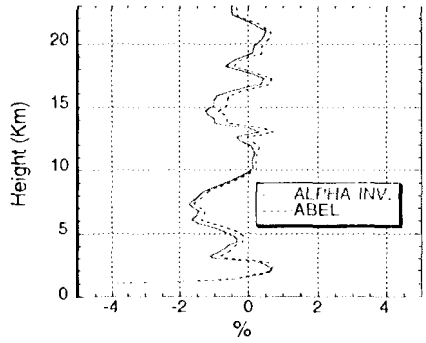

Fig. 2: Fractional refractivity difference between ECMWF analysis and GPS/MET data inverted with the Abel and ALPHA techniques.

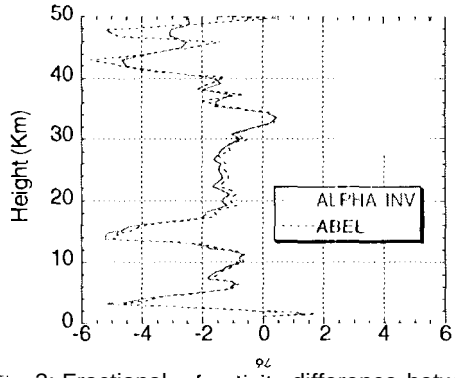

Fig. 3: Fractional refractivity difference between NMC model and GPS/MET data inverted with the Abel and ALPHA techniques.

For each inversion technique, the fractional refractivity difference between GPS/MET and the ECMWF or NMC models are shown. Note that, except at very high altitudes, the Abel and raytracing techniques reproduce nearly the same retrievals with differences in absolute value < (0,1-0.50/0). The larger differences occur near sharp changes in refractivity, where the raytracing routine appears to produce a somewhat smoother retrieval than the Abel inversion, At altitudes above 40 km, differences of about 1-50/. are observed (Fig. 3) between the Abel and ALPHA inversions.

Once refractivity is obtained, then temperature profiles in dry regions (upper troposphere and stratosphere) can be derived from the ideal gas law and hydrostatic equilibrium [Kursinski et al., 1997]. In

addition, if water vapor density is assumed to be known (e.g. based on atmospheric models), then temperature can be derived at heights down to the surface. (In region of high moisture it is more useful to assume knowledge of temperature in the mid- and low-troposphere and solve for water vapor as shown by Kursinski et al., (1995)).

Temperature differences between the NMC model and the Abel and ALPHA inversions are shown in Figure 4, where water vapor in the lower troposphere is assumed to be that of the NMC. An initial value of temperature is needed in order to represent the mass above 50 km in the hydrostatic equilibrium integral and it is taken to be that of the NMC at 50 km, which explains the exact agreements of the retrievals and the model at that height. It was established elsewhere [see e.g. Kursinski et al., 1996; Ware et al., 1996] that temperature accuracy of GPS/MET are <2K between 5-25 km. Larger T differences within these heights in Fig. 4 are reflective of errors in the NMC model. At altitude higher than 30 km (~10 mbar), Fig. 4 shows the ALPHA inversion to agree with NMC to better than 5K.

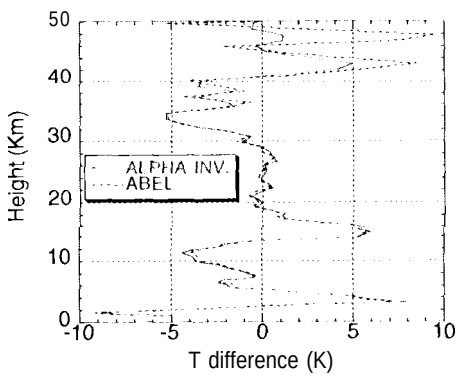

Fig. 4: Temperature difference between NMC and GPS/MET data inverted with Abel and ALPHA techniques

3.2 Receiver Inside The Atmosphere

Positioning a receiver inside the atmosphere, for instance on a mountaintop, tracking the GPS signal down to ther earth's limb, would routinely yield tens of profiles in regions of interest. These profiles would provide much needed vertical information on boundary layer structure.

In order to validate the algorithm's ability to retrieve refractivity when the receiver is inside the atmosphere, we constructed a new set of rneasurements by starting with the occultation data used in the retrievals of Figs. (2-4) and making the changes described as follows. First, we truncated the data set by excluding all measurements with tangent heights > 25 km. Second, we added 12 values of refractivity at heights above 25 km. The values of N used were obtained from the NMC model and extended in heights up to ~60 km. Third, we divided the observed bending angles by 2 and placed the receiver at the tangent point for each link. The rationale behind the last step is that if the atmosphere is exactly spherically symmetric, then a receiver located at the tangent point of the link would measure half the bending that it would measure from space. The situation we created is somewhat similar to carrying a GPS receiver on a balloon that collected GPS measurements up to 25 km altitude. Fig. 5 shows the fractional refractivity difference between the NMC and the ALPHA inversion for the situation when the receiver is inside and outside the atmosphere (the latter is the same as the solid curve of Fig. 3). The almost perfect agreement of NMC and "inside-the-atmosphere" inversion above 30 km is not surprising since it is the NMC refractivity data which is driving the inversion at these heights. However, the fact that the "inside-the-atmosphere" inversion converges very rapidly to the "outside-the-atmosphere" inversion indicates how focused the bending is near the tangent point. As shown by [Kursinski et al., 1997] half of the bending occurs at a height of about 1.5 km above the tangent point, which implies that bending measurements are nearly localized at the layer where the tangent height is. Given that measurements constructed for the "inside-the-atmosphere" retrieval are equivalent to a receiver sitting at 25 km tracking the GPS at negative elevations, Fig. 5 indicates that there is a transition region of about 2-4 km below the receiver where the inversion is dependent on the *a priori* model. This is a large region if we are to apply this technique to a mountain top receiver. However, in the example of Fig. 5, no data from positive elevations were included, which constrains the atmosphere above the receiver and could shorten that transition region to a

few hundreds of meters. The inclusion of positive elevation data is currently being investigated. Temperature retrievals corresponding to Fig. 5 are shown in Fig. 6.

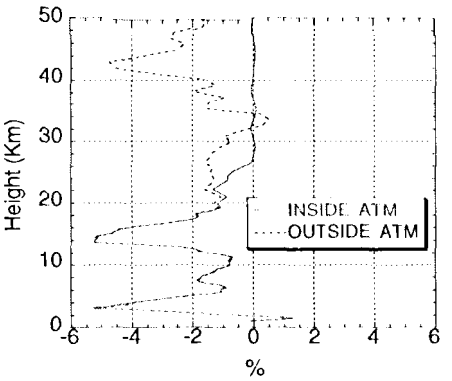

Fig. 5: Fractional refractivity difference between NMC and ALPHA inversion for a receiver inside and outside the atmosphere.

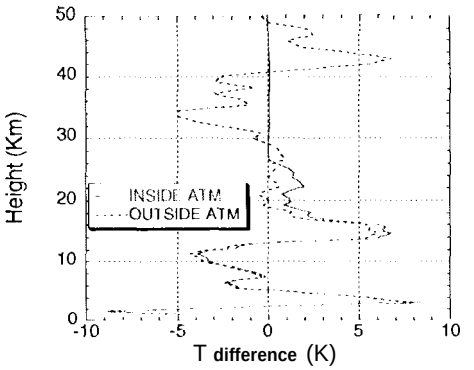

Fig. 6: Temperature differences between NMC and ALPHA inversion for measurements taken from inside and outside the atmosphere.

4. CONCLUSIONS

We have described and demonstrated a technique appropriate for inverting GPS occultation data, which could be used as part of data assimilation into numerical weather models. Even though we have validated this technique assuming a layered exponential model for the atmosphere, it is sufficiently general to be applicable to any one-dimensional atmospheric models, by deriving the computed bending angles and their partial derivatives with respect to the set of model parameters. Conceptually similar work relevant to assimilating GPS occultation data into numerical weather models is also presented in [Eyre, 1994] and [Kuo and Zou, 1996].

Acknowledgments

This work has been performed at the Jet Propulsion Laboratory, Pasadena, under contract with the National Aeronautical and Space Administration, Support from NASA's Mission to Planet Earth Office is gratefully acknowledged.

References

Bierman G. J., (1 977), *factorization Methods for Discrete Sequential Estimation,* Academic Press, Inc., New York.

Eyre J. R. (1994), Assimilation of radio occultation measurements into a numerical weather prediction system, *European Center for Medium-Range Weather Forecasts,* Tech. Memo. No. 199, May.

Fjeldbo G. A. et al. (1971), The neutral atmosphere of Venus as studied with the Mariner V radio occultation experiments, *Astronom, J., 76, No. 2,* pp. *123-140.*

Hajj G. A. et al. (1995), Initial Results of GPS-LEO Occultation Measurements of Earth's Atmosphere obtained with the GPS-MET Experiment, in *GPS Trends in Precise Terrestrial, Airborne, and Spaceborne Applications, G.* Beutler et al. (eds.), Intern. Association of Geodesy Symposia, 115, pp. 144-153.

Kuo Y. H., X. Zou and W. Huang (1996), The impact of GPS data on the prediction of an extra-tropical cyclone: an observing system simulation experiment, submitted to *J. Dyn. Atmos. Ocean,* Feb.

Kursinski E. R. et al. (1995), Observing tropospheric water vapor by radio occultation using the global positioning system, *Geophys. Res. Let.,* Vol. 22, No. 17, pp 2365-2368.

Kursinski E. R., et al. (1996), Initial Results of Radio Occultation Observations of Earth's Atmosphere Using the Global Positioning System, *Science,* Vol. 271, pp. 1107-1110.

Kursinski E. R et al. (1997), Monitoring the Earth's Atmosphere with Radio Occultation Measurements Using GPS, *J. of Geophys. Res.*, to appear.

Tricomi F. G., (1977) *Integral Equations,* Dover Publications, Inc. New York.

Ware R. et al. (1996), GPS Sounding of the Atmosphere from Low Earth Orbit: Preliminary Results, *Bull. Amer. Meteo. Sot.,* Vol. 77 (l), pp. 19-40.